

Intermittent Magnetic Field Excitation by a Turbulent Flow of Liquid Sodium

M. D. Nornberg, E. J. Spence, R. D. Kendrick, C. M. Jacobson, and C. B. Forest*

Department of Physics, University of Wisconsin–Madison, 1150 University Avenue, Madison, Wisconsin 53706, USA

(Received 30 March 2006; published 26 July 2006)

The magnetic field measured in the Madison dynamo experiment shows intermittent periods of growth when an axial magnetic field is applied. The geometry of the intermittent field is consistent with the fastest-growing magnetic eigenmode predicted by kinematic dynamo theory using a laminar model of the mean flow. Though the eigenmodes of the mean flow are decaying, it is postulated that turbulent fluctuations of the velocity field change the flow geometry such that the eigenmode growth rate is temporarily positive. Therefore, it is expected that a characteristic of the onset of a turbulent dynamo is magnetic intermittency.

DOI: [10.1103/PhysRevLett.97.044503](https://doi.org/10.1103/PhysRevLett.97.044503)

PACS numbers: 47.65.-d, 47.65.Md, 91.25.Cw

Determining the onset conditions for magnetic field growth in magnetohydrodynamics is fundamental to understanding how astrophysical dynamos such as the Earth, the Sun, and the Galaxy self-generate magnetic fields. These onset conditions are now being studied in laboratory experiments using flows of liquid sodium [1]. The conditions required for generating a dynamo can be determined by solving the magnetic induction equation

$$\frac{\partial \mathbf{B}}{\partial t} = Rm \nabla \times \mathbf{V} \times \mathbf{B} + \nabla^2 \mathbf{B}, \quad (1)$$

where \mathbf{B} is the magnetic field, \mathbf{V} is the velocity field scaled by a characteristic speed V_0 , and the time is scaled to the resistive diffusion time $\tau_\sigma = \mu_0 \sigma L^2$. The magnetic Reynolds number is $Rm = \mu_0 \sigma L V_0$, where σ is the conductivity of the fluid and L is a characteristic scale length [2]. In the kinematic approximation, the velocity field is assumed to be a prescribed flow (either the flow is stationary or its time dependence is specified), and Lorentz forces due to the magnetic field are neglected. Equation (1) is then linear in \mathbf{B} and can be solved as an eigenvalue problem. Several different types of stationary, helical flows have been shown theoretically to be kinematic dynamos [3–6], which in turn has led to the design of current dynamo experiments. For particular flows, the kinematic model predicts a critical value of the magnetic Reynolds number Rm_{crit} , above which the magnetic field becomes linearly unstable; i.e., for $Rm > Rm_{\text{crit}}$ a small seed magnetic field will grow exponentially in time. The dynamo onset conditions have been tested in helical pipe-flow experiments at Riga [7,8] and Karlsruhe [9,10]. Both experiments generated magnetic fields at a value of Rm_{crit} consistent with predictions from the kinematic theory.

Fluids and plasmas such as the Earth's liquid core, the solar convection zone, and liquid metals are turbulent under the conditions required for a dynamo. The Riga and Karlsruhe experiments use highly constrained flows to create the helical geometry necessary for magnetic field generation. Astrophysical dynamos, however, are often generated by flows in simply connected geometries which

do not exhibit the scale separation between the large-scale magnetic field and the fluctuating part of the velocity field employed in the Riga and Karlsruhe experiments. This discrepancy has prompted the creation of several experiments to investigate the dynamo onset conditions in simply connected flows with fully developed turbulence [11–13].

The threshold for the dynamo instability is not expected to be the smooth transition from decaying to growing magnetic fields described by laminar kinematic theory [14]. Large-scale eddies can cause the instantaneous flow to differ significantly from the mean flow. The growth rate of the magnetic field is highly sensitive to the flow geometry, and so the instantaneous flow may occasionally satisfy $Rm > Rm_{\text{crit}}$ while the mean flow does not. The fastest-growing global magnetic eigenmode would then fluctuate between growing and decaying states. The threshold of magnetic field growth, therefore, has a range characterized by intermittent bursts of magnetic field growth. In this Letter, the observation of an intermittently excited magnetic field in a simply connected, turbulent flow of liquid sodium is reported. The structure of the excited field is consistent with the largest-growing magnetic eigenmode predicted from a laminar kinematic model of the mean flow.

The Madison dynamo experiment [Fig. 1] is a 1 m diameter stainless steel sphere filled with liquid sodium [15]. Results presented in this Letter are from a turbulent two-vortex flow, similar to the flows described in Ref. [6], created by two counterrotating impellers. The impellers are each driven by 75 kW motors and can achieve rotation rates up to 25 Hz, corresponding to $Rm_{\text{tip}} = \mu_0 \sigma L V_{\text{tip}} = 150$ based on the impeller tip speed.

The mean flow is designed to generate growing magnetic fields according to a laminar kinematic dynamo model [11]. According to the kinematic eigenvalue calculations, for sufficiently large Rm the experimental flow is expected to excite a dipole magnetic field oriented transverse to the symmetry axis [Fig. 1]. An array of 74 temperature-compensated Hall probes on the surface

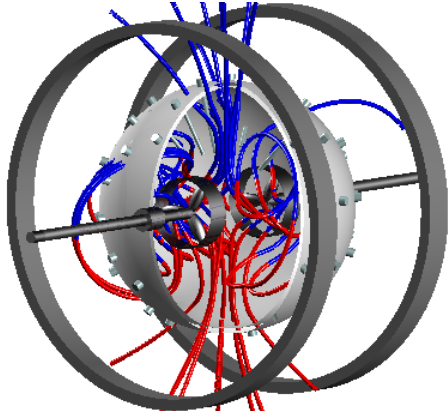


FIG. 1 (color online). A schematic of the Madison dynamo experiment with superimposed magnetic field lines of the theoretically predicted dominant magnetic eigenmode.

of the sphere provides measurements of the instantaneous multipole structure of the magnetic field induced by currents in the liquid sodium. The Hall probes are capable of resolving changes in the magnetic field down to 0.3 G with a maximum range of ± 170 G. A pair of magnetic field coils coaxial with the axis of rotation are used to apply a nearly uniform 50 G axial field. This seed field brings the field induced by the flow above the noise level of the Hall probes. The applied field is sufficiently small that the strength of the Lorentz force is about 1% of the fluid inertial forces.

The velocity field of an identical-scale water model of the experiment is measured using laser Doppler velocimetry (LDV) [15]. The velocity measurements have Gaussian probability distribution functions (PDFs) [Fig. 2(a)] as expected from a stationary turbulent flow according to the central limit theorem [16]. The magnetic fluctuations measured near the axis of symmetry of the sodium experiment also have Gaussian distributions [Fig. 2(b)]. In addition to these normally distributed fluctuations, there are

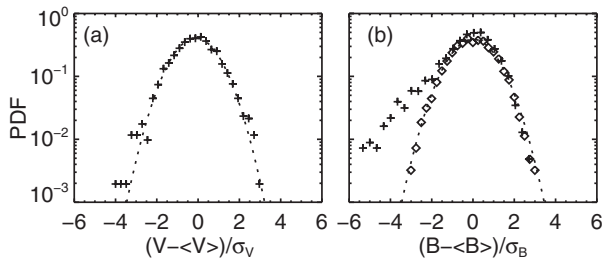


FIG. 2. (a) PDF constructed from LDV measurements of v_ϕ in the water model of the experiment (+) with a Gaussian fit (dotted line). The difference between v_ϕ and its mean is scaled to the standard deviation σ_V . (b) PDF constructed from B_r measurements in the sodium experiment near the equator (+) and near the symmetry axis (\diamond) with a Gaussian fit (dotted line). The difference between B_r and its mean is scaled to the standard deviation σ_B .

intermittent, large-amplitude magnetic bursts observed on probes near the equator of the experiment. The magnetic field during a burst has the spatial structure expected from the least-damped magnetic eigenmode from kinematic theory [Fig. 3]. The orientation of the transverse dipole is random for each burst so that the time-averaged induced field is axisymmetric.

The bursts are ensemble averaged to determine typical characteristics. A burst is defined to occur when the energy in the transverse dipole field exceeds a certain threshold. For this analysis, the threshold is 50% of the maximum energy of the time series [Fig. 4]. This threshold is sufficiently small to capture a large number of bursts yet significantly larger than the mean energy (about 2 standard deviations above the mean energy for each time series). The bursts are averaged together, and the growth rate is determined by an exponential curve fit [Fig. 5]. The results for various impeller rotation rates are reported in Table I. It should be noted that the strength of the fluctuations in the field is at most equal to the on-axis applied field strength of 50 G; hence, the Lorentz force due to the fluctuations is weak compared to inertial forces.

There are several possible mechanisms for the excitation of the transverse dipole field. Velocity field fluctuations are large, with $\tilde{V}/\langle V \rangle \approx 0.5$ as determined from LDV measurements. These large fluctuations cause the peak flow speed to vary, which can be interpreted as variation in Rm . Fluctuations at the largest scales can also cause changes in the shape of the flow leading to variation of Rm_{crit} . The statistics of the small-scale fluctuations could change, also contributing to variation of Rm_{crit} . If the kinetic helicity of the small-scale eddies becomes sufficiently strong, the net current generation could give rise to the observed magnetic field bursts [17,18]. Regardless of scale, subtle changes in the flow can adjust the instability threshold.

To estimate the likelihood that the flow is self-exciting, the kinematic growth rate from the velocity field measured in the water experiment is calculated [Fig. 6]. The solid line shows the results of the calculation using the mean

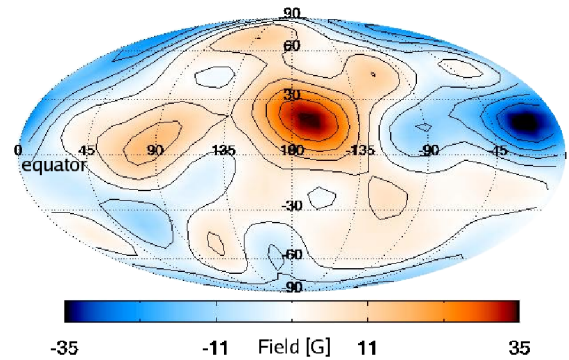


FIG. 3 (color online). Contours of $B_r(\theta, \phi)$ measured on the surface of the sphere. The applied field is subtracted from the measurements. This snapshot of the measured field corresponds to an induced dipole field transverse to the drive shaft axis.

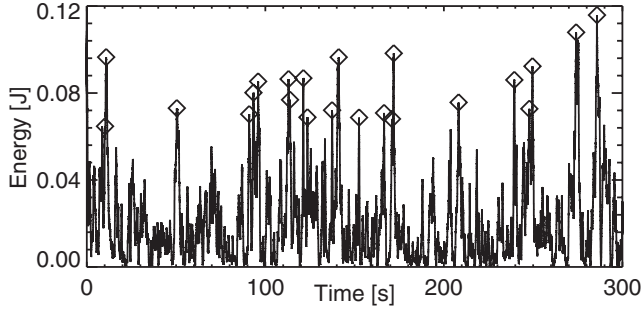


FIG. 4. Time series of the energy in the transverse dipole field for an impeller rotation rate of 10 Hz. The diamonds mark the peak of a burst where the energy exceeds 50% of its maximum value.

flow, whereas the dashed line shows the growth rate calculated for an optimized flow geometry similar to and within the fluctuation levels of the measured flow [14]. The region between the growth rates of the mean and optimized flows indicates the range of possible eigenmode growth rates for an instantaneous realization of the flow and the resulting variation in Rm_{crit} .

The velocity fluctuations also contribute to variations in the instantaneous maximum speed of the flow, thereby creating a range of Rm . Probability distributions of Rm constructed from the measured velocity fluctuations for three different impeller rotation rates are plotted in Fig. 6. It is expected that a greater overlap of the PDF of Rm with the range of Rm_{crit} will result in magnetic field excitations with greater frequency and strength. The duration of each excitation is expected to decrease, since the correlation time of the velocity fluctuations scales as $\tau_c \sim \ell/V_\ell$ where ℓ is the eddy scale length and V_ℓ is the characteristic speed of the eddy. For example, LDV measurements from the water model give $\tau_c = 80 \pm 20$ ms for the $f_{tip} = 16.7$ Hz flow, consistent with eddies of size $\ell = 0.25$ m and speed $V_\ell = 3$ m/s. The proportion of time that the magnetic field is bursting is estimated to be $n_d = f_b \tau_b$, where f_b is the average frequency of the bursts and τ_b is the width of the conditionally averaged burst at half maxi-

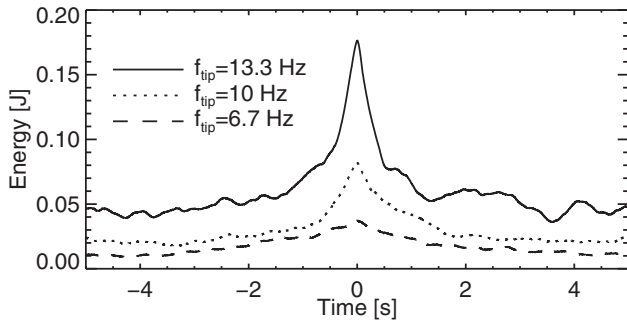


FIG. 5. The ensemble average of bursts from three time series. The averaged burst is used to calculate the growth rate and burst width in Table I.

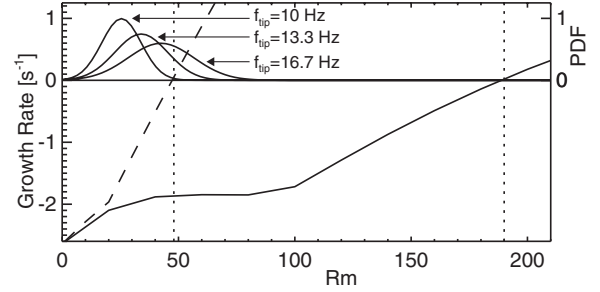


FIG. 6. Kinematic growth rate versus Rm for the mean flow measured in the water experiment (solid line) and an optimized flow (dashed line). The vertical lines identify Rm_{crit} for each case. The PDFs of Rm for flows with three different impeller rotation rates are shown to demonstrate the increasing overlap of the ranges of Rm and Rm_{crit} .

um. The data in Table I show that the proportion of time the flow is bursting stays relatively constant between 5% and 8%.

Table I reveals that the standard deviation of the energy in the intermittent transverse dipole field is approximately equal to its mean value, a characteristic of a Poisson probability distribution [19]. Assuming each excitation can be treated as a rare random event, the probability distribution of the magnetic field energy can be determined heuristically. The probability of measuring n bursts in time t is given by $P(t) = (f_b t)^n e^{-f_b t} / n!$, where f_b is the average rate of bursts. The average growth of the magnetic field over time t during a burst is $\Delta B = B_0 e^{\lambda t}$, where B_0 is the average strength of the initial seed field. The resulting gain in the magnetic field energy per unit volume is $\Delta E = \Delta B^2 / 2\mu_0 = (B_0^2 / 2\mu_0) \exp(2\lambda t)$, and so $t = \log(\Delta E / E_0) / 2\lambda$, where $E_0 = B_0^2 / 2\mu_0$. Substituting the time in terms of ΔE into the Poisson distribution yields a log-Poisson distribution for the probability density of ΔE :

$$P(\Delta E) = \frac{1}{n!} \left[\frac{f_b}{2\lambda} \ln\left(\frac{\Delta E}{E_0}\right) \right]^n e^{-(f_b/2\lambda) \ln(\Delta E/E_0)}. \quad (2)$$

TABLE I. The magnetic Reynolds number Rm based on the maximum speed in measured flows, duration of the measurement T , number of bursts N_b , average burst rate f_b , burst width τ_b , growth rate λ_b , estimate of the overall fraction of time the flow is bursting n_d , mean energy $\langle E \rangle$, and standard deviation of the energy σ_E as a function of the rotation rate of the impellers f_{tip} .

f_{tip} [Hz]	Rm	T [s]	N_b	f_b [s ⁻¹]	n_d [%]	τ_b [s]	λ_b [s ⁻¹]	$\langle E \rangle$ [mJ]	σ_E [mJ]
3.3	14	300	5	0.017	6.7	3.99	0.17	2	2
6.7	22	300	9	0.030	7.5	2.50	0.30	9	8
10.0	28	300	22	0.070	6.1	0.83	1.12	21	20
13.3	35	300	38	0.127	7.3	0.58	1.62	48	43
16.7	42	300	37	0.123	6.3	0.51	2.22	78	76
20.0	49	100	15	0.150	5.4	0.36	2.93	111	98

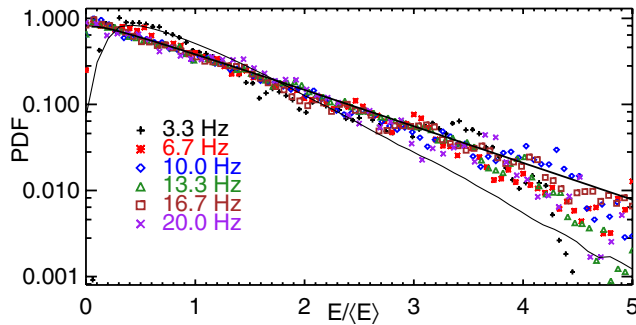


FIG. 7 (color online). The PDF of the energy in the transverse dipole field for several impeller rotation rates. The thick line is an example Poisson distribution. The thin line represents the energy distribution if the magnetic fluctuations were Gaussian.

The probability distributions of the transverse dipole energy are shown in Fig. 7. The distributions with large numbers of bursts tend to have significantly more high energy fluctuations than expected from Gaussian fluctuations. The overall invariance of the distributions as the impeller rotation rate is increased demonstrates that the increased frequency of bursts is offset by their shortened duration.

The results presented demonstrate how turbulence in a simply connected geometry changes the onset conditions of the dynamo. Rather than the smooth transition from damped to growing fields predicted by either kinematic or mean field dynamo theory, the transition is characterized by intermittent magnetic field bursts, which may be relevant to some dynamo models [20]. Although sustained growth is not yet observed, the transient excitation demonstrates the intermittent characteristics of a turbulent dynamo.

The authors thank S. A. Boldyrev and E. G. Zweibel for their helpful suggestions and C. A. Parada for his assistance in the experiments. This work is funded by the Department of Energy, the National Science Foundation, and the David and Lucille Packard Foundation.

*Electronic address: cbforest@wisc.edu

- [1] A. Gailitis, O. Lielausis, E. Platacis, G. Gerbeth, and F. Stefani, *Rev. Mod. Phys.* **74**, 973 (2002).
- [2] H. K. Moffatt, *Magnetic Field Generation in Electrically Conducting Fluids* (Cambridge University Press, Cambridge, England, 1978).
- [3] Y. B. Ponomarenko, *J. Appl. Mech. Tech. Phys.* **14**, 775 (1973).
- [4] D. Gubbins, *Phil. Trans. R. Soc. A* **274**, 493 (1973).
- [5] F. H. Busse, *Geophys. J. R. Astron. Soc.* **42**, 437 (1975).
- [6] M. L. Dudley and R. W. James, *Proc. R. Soc. A* **425**, 407 (1989).
- [7] A. Gailitis *et al.*, *Phys. Rev. Lett.* **84**, 4365 (2000).
- [8] A. Gailitis *et al.*, *Phys. Rev. Lett.* **86**, 3024 (2001).
- [9] R. Stieglitz and U. Müller, *Phys. Fluids* **13**, 561 (2001).
- [10] U. Müller, R. Stieglitz, and S. Horany, *J. Fluid Mech.* **498**, 31 (2004).
- [11] C. B. Forest *et al.*, *Magnetohydrodynamics* **38**, 107 (2002).
- [12] F. Pétrélis *et al.*, *Phys. Rev. Lett.* **90**, 174501 (2003).
- [13] D. P. Lathrop, W. L. Shew, and D. R. Sisan, *Plasma Phys. Controlled Fusion* **43**, A151 (2001).
- [14] R. O'Connell *et al.*, in *Dynamo and Dynamics, a Mathematical Challenge*, edited by P. Chossat, D. Ambruster, and I. Oprea, NATO Science Series II, Mathematics, Physics and Chemistry Vol. 26 (Kluwer Academic, Dordrecht, 2000), pp. 59–66.
- [15] M. D. Nornberg, E. J. Spence, R. D. Kendrick, C. M. Jacobson, and C. B. Forest, *Phys. Plasmas* **13**, 055901 (2006).
- [16] H. Tennekes and J. L. Lumley, *A First Course in Turbulence* (MIT, Cambridge, MA, 1972).
- [17] E. J. Spence, M. D. Nornberg, C. M. Jacobson, R. D. Kendrick, and C. B. Forest, *Phys. Rev. Lett.* **96**, 055002 (2006).
- [18] F. Cattaneo and S. M. Tobias, *Phys. Fluids* **17**, 127105 (2005).
- [19] L. D. Landau and E. M. Lifshitz, *Statistical Physics* (Reed Educational and Professional Publishing, Oxford, 1999).
- [20] C. M. Ko and E. N. Parker, *Astrophys. J.* **341**, 828 (1989).